

Current reversal in collective ratchets induced by lattice instability

L. Dinis,¹ E.M. González,² J.V. Anguita,³ J.M.R. Parrondo,¹ and J.L. Vicent²

¹*Departamento de Física Atómica, Molecular y Nuclear and GISC,
Universidad Complutense de Madrid, 28040-Madrid, Spain*

²*Departamento de Física de Materiales, Universidad Complutense de Madrid, 28040-Madrid, Spain*

³*Instituto de Microelectrónica de Madrid, Consejo Superior de Investigaciones Científicas, Tres Cantos, 28670-Madrid, Spain*
(Dated: October 30, 2018)

A collective mechanism for current reversal in superconducting vortex ratchets is proposed. The mechanism is based on a two-dimensional instability of the ground state ($T = 0$) of the system. We illustrate our results with numerical simulations and experiments in Nb superconducting films fabricated on top of Si substrates with artificially induced asymmetric pinning centers.

PACS numbers: 05.40.-a, 02.30.Yy, 74.25.Qt, 85.25.-j

I. INTRODUCTION

Rectification of motion and fluctuations in the nanoscale is becoming a major field of research¹. Rectifying mechanisms or *ratchets* have been used to explain how protein motors work^{2,3} and to design new separation techniques⁴ or synthetic chemical motors^{5,6}. Superconductors have become a powerful tool to study ratchet mechanisms⁷. Recently, a superconducting vortex ratchet device has been reported by Villegas et al⁸. In that experiment, the rocking ratchet mechanism is due to a superconducting film patterned with a lattice of asymmetric potentials acting as pinning centers. An input ac current yields an output dc voltage in the superconducting film, revealing a rich phenomenology of single and multiple current reversals^{8,9,10}, very sensitive to the underlying vortex dynamics. The interest of vortex ratchets is then twofold: it reveals new collective rectification mechanisms and sheds light on the physics of vortices in superconductors.

Current reversals in vortex ratchets have been explained, in the framework of one-dimensional models, by the coexistence of pinned and interstitial vortices moving in opposite directions⁸ or by the interaction between vortices within the pinning centers in one-dimensional channels⁹. Olson and Reichhardt¹¹ have studied numerically a two-dimensional model, obtaining current reversal only when interstitial vortices are present in the ground state. They provide intuitive explanations of different rectification mechanisms based on local interactions between vortices and pinning centers.

In this Letter we experimentally show that current reversal can also occur when interstitial vortices are absent in the ground state ($T=0$). Remarkably, current reversal disappears increasing either the pinning strength or the temperature. We also present numerical simulations of vortices as interacting Brownian particles in two dimensions, indicating that this current reversal is due to a new collective effect: an instability of the ground state, selective to the sign of the applied force. The influence of lattice instabilities on rectification has been also recently analyzed by Lu et al.¹², for two dimensional vortices in

a substrate with a one-dimensional modulation.

II. EXPERIMENTAL RESULTS

For our experiments, two types of asymmetric pinning centers have been fabricated: magnetic (Ni) nanotriangles and non-magnetic (Cu) nanotriangles. The vortex pinning force is enhanced by magnetic centers in comparison with non-magnetic centers¹³. The nanotriangles were fabricated using e-beam lithography techniques and Si (100) wafers as substrates. The Ni or Cu arrays of nanotriangles, on top of the substrate, are covered with a sputtered Nb thin film. Ni or Cu thickness (triangles height) is 40 nm and Nb film is 100 nm thick. Further details on this fabrication technique can be found elsewhere¹⁴. For the present work, we have fabricated arrays with the same nanotriangle dimensions and array periodicity than those in Ref. 8.

We have measured magnetotransport in these films using a commercial He cryostat. The variable temperature insert allows controlling temperature with stability of 1 mK. For these experiments, samples were patterned with a cross-shaped measuring bridge⁸, by using optical lithography and ion-etching. This patterned bridge allows us to control the Lorentz force on the vortices in the mixed state: taking into account $\vec{F}_L = \vec{J} \times \vec{n} \phi_0$ (with $\phi_0 = 2.07 \times 10^{-15}$ Wb and \vec{n} a unitary vector parallel to the applied magnetic field). On the other hand, from the expression for the electric field $\vec{E} = \vec{B} \times \vec{v}$, where \vec{B} is the applied magnetic field and \vec{v} the vortex-lattice velocity, we can calculate this velocity $v = V/(dB)$ from the measured voltage drops V (d being the distance between contacts). See Ref. 8 for more experimental details.

The dc magnetoresistance in the mixed state of samples with periodic arrays of pinning centers exhibits well-known commensurability phenomena^{15,16}, in which minima develop as a consequence of geometrical matching between the vortex-lattice and the underlying periodic structure. These minima are equally spaced (two neighbor minima are always separated by the same magnetic field value). For example, in the case of square arrays

of nanostructured pinning centers, minima appear at applied magnetic fields $H_m = n(\phi_0/a^2)$, where a is the lattice parameter of the square array. Hence, the number of vortices n per array unit cell can be known by simple inspection of the dc magnetoresistance $R(H)$ curves. Moreover, for non-magnetic pinning centers Mkrtychyan and Shmidt¹⁷ have given a rough estimation of the maximum number of vortices that can be pinned in each center, which could confirm the matching field minima values. This filling factor can be calculated as the ratio between half the dimension of the pinning center (the triangle side is around 650 nm)⁸ and two times the superconducting coherence length (around 60 nm for these samples and temperatures close to the critical temperature)¹⁶. In our samples this rough estimation gives us approximately three vortices per triangle, in agreement with the matching field data (see also 8). Therefore, we know, for selected values of the applied magnetic field, how many vortices there are per unit cell and where they are, this is, if they are interstitial vortices or vortices in the pinning centers.

We want to underline that collective behavior of vortices in films with periodic pinning is crucial to understand vortex lattice reconfiguration effects¹⁸ or vortex channeling¹⁹. Also, collective effects in ratchets have been shown to yield new interesting phenomena²⁰.

Measurements of the vortex lattice average velocity as a function of the applied force are depicted in Fig. 1(a) for sample (A), Ni triangles, and three vortex per triangle ($n = 3$). There is no current reversal in the rectified signal in agreement with the explanation given in Ref. 8 (see below). Experiments for sample (B), Cu triangles, also for $n = 3$ (Fig. 1(b)) show a similar behavior for $T = 8.165\text{K}$ ($T = 0.99 T_c$), but a current reversal appears decreasing the temperature, despite the fact that there are still three vortices per triangle.

In the one-dimensional approach reported in Ref. 8, the vortex lattice does not play any role, and the current reversal was explained assuming that pinned and interstitial vortices are rectified in opposite directions. However, this assumption fails to explain current reversal for the matching field $n = 3$, since in this case there are no interstitial vortices in the ground state of the system. The simulations performed by Olson and Reichardt¹¹ do not exhibit any current reversal for $n = 3$ and the rectification mechanisms that they propose do not apply for this case either. Therefore, a new explanation of current reversal is required. We have found by numerical simulations such an explanation based on the interplay between the vortex lattice and the geometry of the triangular defects.

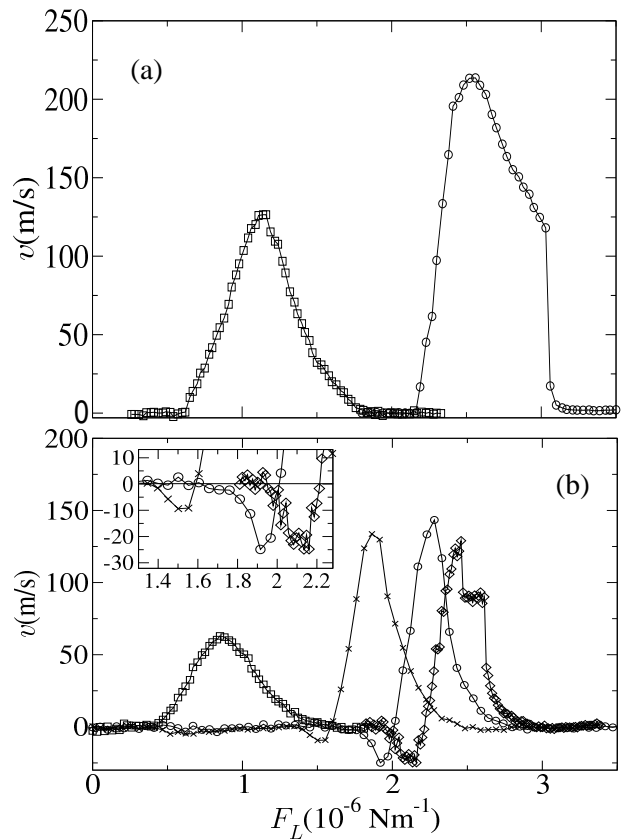


FIG. 1: Net velocity of vortices versus ac Lorentz force amplitude ($\omega = 10\text{kHz}$). Array periodicity 770 nm, triangle base 620 nm. (a) Sample (A): Nb film with Ni triangles $T_c = 8.35\text{K}$, $T/T_c = 0.99$ ($T = 8.265\text{K}$) (\square), $T/T_c = 0.98$ ($T = 8.174\text{K}$) (\circ). (b) Sample (B): Nb film with Cu triangles $T_c = 8.24\text{K}$. $T = 8.165\text{K}$ (\square), $T = 8.102\text{K}$ (\times), $T = 8.08\text{K}$ (\circ), $T = 8.065\text{K}$ (\diamond). The negative velocity part of each curve is shown in the inset.

III. THEORETICAL MODEL

A. Simulations

The simulations have been performed by numerically solving Langevin equations for the movement of the vortices

$$\eta \dot{\mathbf{x}} = -\partial_x U_{vv} + \nabla V_p + \mathbf{F}_{\text{ext}} + \xi(t). \quad (1)$$

\mathbf{F}_{ext} is the Lorentz force resulting from the applied current, U_{vv} the usual vortex-vortex interaction (see Ref.²¹), V_p the pinning potential, η the friction coefficient, and $\xi(t)$ a white gaussian thermal noise. The pinning force and vortex-vortex interaction must be in agreement with the experimental situation of three vortices per pinning site (triangle). The interaction of the vortices with the pinning defects is modelled by a potential V_p in the shape of a triangle and with a hyperbolic tangent profile. The depth of the potential is $V_{p0} = 0.002 \text{ pN}\mu\text{m}$,

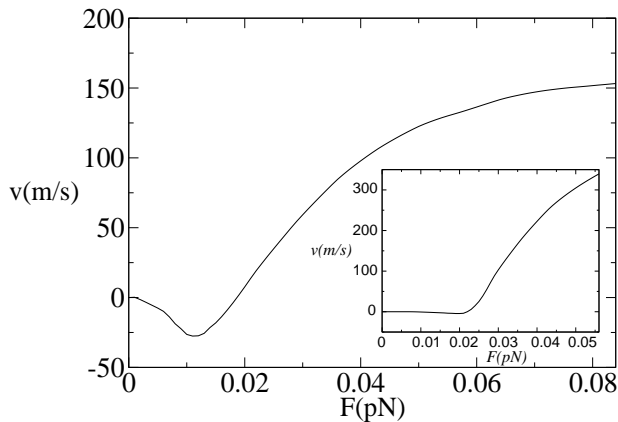


FIG. 2: Simulation results. Three vortices per triangle, pinning $0.002 \text{ pN } \mu\text{m}$. Inset: pinning $0.0036 \text{ pN}\mu\text{m}$.

so that depinning forces have typical values of the order of 10^{-6} N/m . Experiments^{22,23} show that the system is adiabatic in the region of frequencies used. This allows us to obtain the expected ac signal from the velocity-force response curves obtained in simulations, both for constant positive and negative applied force.

Results are shown in Fig. 2 where a window of downward rectification can be observed. Let us stress at this point that the “natural” direction of rectification for pinned vortices is upwards. The reason is that the vortex feels a smaller force at the tip of the triangle than at the triangle base. The force at the tip can be, for an equilateral triangle, as lower as half the force at the base of the triangle.

B. Ground state instability

What is then the origin of the downward rectification for small forces? Our simulations indicate that the rectification is due to a two-dimensional instability of the ground state under small downward forces. The ground state of the system consists of vortices located in the corners of each triangle, without interstitial vortices. However, for finite temperature, there are some “defective triangles” in the actual configuration of vortices, i.e., some triangles which have only two vortices inside. Accordingly, some interstitial vortices will be randomly spread along the sample. Fig. 3 shows one of these configuration with only one defective triangle out of 6×6 . For low forces, motion is induced by the interstitial vortices *both* in the downward and upward direction. However, contrary to the picture presented in previous works⁸, there is not a continuous motion of interstitial vortices along the space between triangles: the interstitial vortex enters the nearest triangle expelling one of the three vortices inside.

The aforementioned instability, selective to the sign of the external force, is shown in Fig. 3. We have chosen an initial condition with only one interstitial vortex and one

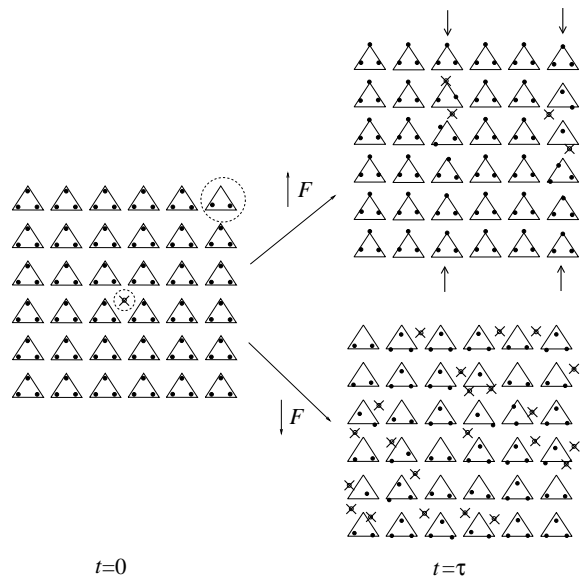


FIG. 3: Downward rectification mechanism at $T = 0 \text{ K}$: snapshots from simulations. Initial condition (left) and configurations after evolution ($\tau = 6.5 \times 10^{-9} \text{ s}$) with positive force $F = 0.032 \text{ pN}$ (right, up) and negative force $-F$ (right, down). Dashed circles show the defective triangle and the only interstitial present in the initial condition. Thick arrows point out the only two columns presenting any motion when positive force is applied. Comparison of the right panels shows that the number of interstitial vortices (\times) dramatically increases when the external force points downwards.

defective triangle, located at some distance. In the right figures we have plotted the configurations of vortices after an upward and downward force has been applied for $\tau = 6.5 \times 10^{-9}$ seconds (long enough for a depinned vortex to cover the whole sample several times), respectively. This simulations evolved at zero temperature to show the mechanism in a clearer manner. We see that, in the case of the upward force, the interstitial vortex remains in *one single column*. The column with a defective triangle also moves, but again vortices remain in that column. As a consequence, there is a positive current of vortices but the motion is constrained to two columns. When the interstitial vortex enters a triangle, the top vortex in the triangle moves upwards, out of it and into the following one. In addition to that, in the defective triangle, one of the two vortices always escapes through the tip, becoming an interstitial vortex and triggering a process similar to that in the column with an extra vortex. Both motions propagate along the column without disturbing the neighboring columns.

On the other hand, under a downward force, the initial defect in the ground state propagates along the whole sample, as it is clearly shown in Fig. 3. A more detailed analysis of the simulations show that, when an interstitial vortex enters a triangle, one of the two bottom vortices is expelled but now can move to a triangle *in one of the nearest columns*. It even happens frequently that the two

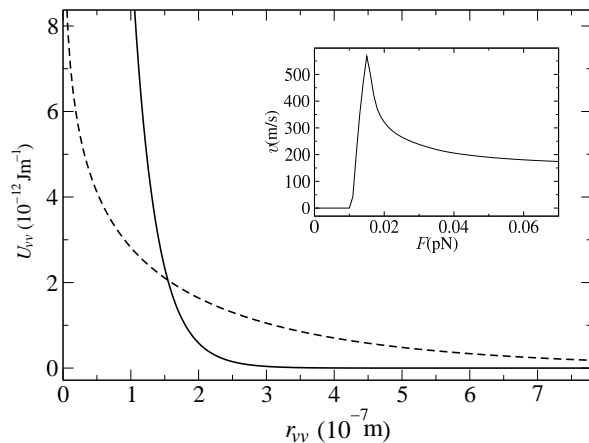


FIG. 4: Vortex-vortex interaction versus vortex-vortex distance. Solid line: interaction used in simulations corresponding to current reversal (see Fig. 2, pinning $V_{p0} = 0.002\text{pN}\mu\text{m}$). Dashed line: interaction used in simulations showing no current reversal, which are depicted in the inset (pinning $V_{p0} = 0.002\text{pN}\mu\text{m}$).

vortices in the base of the triangle are depinned. Consequently, the initial defect is then spread out along the horizontal direction, yielding a considerable large fraction of depinned vortices which increase the overall motion in the system, yielding a net downward rectification and the corresponding current reversal.

As was noted before, current inversion may disappear when the pinning potential is increased. This effect was observed in experiments where the Cu triangles were replaced by Ni ones which have a higher pinning strength (see Fig. 1(a)), and it is also reproduced in our simulations. Results for pinning potential $V_{p0} = 0.0036\text{pN}\mu\text{m}$ do not show current reversal, as depicted in the inset in Fig. 2. The increased pinning strength implies that a larger force is needed to depin vortices when pushing downwards. According to simulations, when the same

force is applied upwards, the aforementioned columnar movement starts, but also neighboring columns without defective triangles or extra vortices depin, and eventually motion spreads all over the sample. In other words, for these moderate values of the force, the instability appears in both directions.

Finally, current reversal in sample (B), Cu triangles, also vanishes when temperature is raised (see Fig. 1(b)). We can explain this behavior taking into account that the penetration depth of the superconductor increases with temperature. As a result, the vortex-vortex interaction strength, U_{vv} , decreases at short distance but its range becomes longer²¹, as depicted in Fig. 4. In this case we observe that the long range vortex lattice order precludes the instability responsible for current reversal (see the inset in Fig. 4).

IV. CONCLUSIONS

In summary, our simulations show that the asymmetric substrate induces an instability sensitive to the direction of the external force, affecting rectification. This effect can explain the current reversal observed in our experiments for $n = 3$. Moreover, our work indicates that the lattice configuration, and consequently its dynamical properties, can be controlled by external forces. This interplay between rectification, driving forces and lattice configuration can induce other interesting phenomena such as transitions between different lattice configurations¹⁰, and could help to design new rectifying devices, not only in superconducting films, but also in other two dimensional collective systems, such as Josephson arrays or colloidal suspensions.

We acknowledge support by Spanish Ministerio de Educación y Ciencia (NAN04-09087, FIS05-07392, MAT05-23924E, MOSAICO), CAM (S-0505/ESP/0337) and UCM-Santander. Computer simulations were performed at “Cluster de cálculo para Técnicas Físicas” of UCM, funded in part by UE-FEDER program and in part by UCM and in the “Aula Sun Microsystems” at UCM.

¹ P. Reimann, Phys. Rep. **361**, 57-265 (2002); Special issue ed. by H. Linke, Appl. Phys. A: Mater. Sci. Process. **75**, 167 (2002).

² G. Bar-Nahum, V. Epshtein, A.E. Rukenstein, R. Rafikov, A. Mustaev and E. Nudler, Cell **120**, 183-193 (2005).

³ J.C.M. Gebhardt, A.E.M. Clemen, J. Jaud, and M. Rief, Proc. Nat. Ac. Sci. **103**, 8680 (2006).

⁴ J. Rousselet, L. Solome, A. Ajdari, and J. Prost, Nature **370**, 446 (1994).

⁵ V. Serreli, C.F. Lee, E.R. Kay, and D.A. Leigh, Nature **445**, 523 (2007).

⁶ T.J. Huang, B. Brough, C.M. Hoa, Y. Liu, A.H. Flood, P.A. Bonvallet, H.R. Tseng, J. F. Stoddarta, M. Baller, and S. Magonov, Appl. Phys. Lett. **85**, 5391 (2004).

⁷ I. Zapata, R. Bartussek, F. Sols, and P. Hänggi, Phys. Rev. Lett. **77**, 2292 (1996); C. S. Lee, B. Janko, L. Derényi, and

A. L. Barábasi, Nature **400**, 337 (1999); J. F. Wambaugh, C. Reichhardt, C. J. Olson, F. Marchesoni, and F. Nori, Phys. Rev. Lett. **83**, 5106 (1999).

⁸ J.E. Villegas, S. Savelev, F. Nori, E.M. Gonzalez, J.V. Anguita, R. Garcia, and J.L. Vicent, Science **302**, 1188 (2003).

⁹ C. C. de Souza Silva, J. V. de Vondel, M. Morelle, and V. V. Moshchalkov, Nature **440**, 651 (2006).

¹⁰ L. Dinis, E.M. Gonzalez, J.V. Anguita, J.M.R. Parrondo, and J.L. Vicent, New J. Phys. **9**, 366 (2007).

¹¹ C. J. Olson-Reichhardt, and C. Reichhardt, Physica C **432**, 125 (2005).

¹² Q. Lu, C.J. Olson Reichhardt, and C. Reichhardt, Phys. Rev. B **75**, 054502 (2007).

¹³ Y. Jaccard, J. I. Martin, M. C. Cyrille, M. Velez, J. L. Vicent, and I. K. Schuller, Phys. Rev. B **58**, 8232 (1998).

- ¹⁴ J. I. Martín, Y. Jaccard, A. Hoffmann, J. Nogues, J. M. George, J. L. Vicent, and I. K. Schuller, *J. Appl. Phys.* **84**, 411 (1998).
- ¹⁵ O. Daldini, P. Martinoli, J.L. Olsen, G. Berner, *Phys. Rev. Lett.* **32**, 218 (1974); A. Pruymboom, P.H. Kes, E. van der Drift, S. Radelaar, *Phys. Rev. Lett.* **60**, 1430 (1988); Y. Otani, B. Pannetier, J.P. Nozières, D. Givord, *J. Magn. Mater.* **126**, 622 (1993); M. Baert, V. Metlushko, R. Jonckheere, V.V. Moshchalkov, and Y. Bruynseraede, *Phys. Rev. Lett.* **74**, 3269 (1995); D.J. Morgan, J.B. Ketterson, *Phys. Rev. Lett.* **80**, 3614 (1998).
- ¹⁶ J.I. Martín, M. Vélez, J. Nogués, I.K. Schuller, *Phys. Rev. Lett.* **79**, 1929 (1997).
- ¹⁷ G.S. Mkrtychyan and V.V. Shmidt, *Sov. Phys. JETP* **34**, 195 (1972).
- ¹⁸ J.I. Martín, M. Vélez, A. Hoffmann, Ivan K. Schuller, and J. L. Vicent, *Phys. Rev. Lett.* **83**, 1022 (1999).
- ¹⁹ M. Vélez, D. Jaque, J.I. Martín, M.I. Montero, I.K. Schuller, J.L. Vicent, *Phys. Rev. B* **65**, 104511 (2002).
- ²⁰ F. Jülicher, A. Ajdari, and J. Prost, *Rev. Mod. Phys.* **69**, 1269 (1997); P. Reimann, R. Kawai, C. Van den Broeck, and P. Hänggi, *Europhys. Lett.* **45**, 545 (1999); F.J. Cao, L. Dinis, and J.M.R. Parrondo, *Phys. Rev. Lett.* **93**, 040603 (2004).
- ²¹ M. Tinkham, *Introduction to Superconductivity*, second ed. (McGraw-Hill, New York, 1996) p. 154.
- ²² J.E. Villegas, E.M. Gonzalez, M.P. Gonzalez, J.V. An-guita, and J.L. Vicent, *Phys. Rev. B* **71**, 024519 (2005).
- ²³ J. Van de Vondel, C.C. de Souza Silva, B.Y. Zhu, M. Morelle, and V. V. Moshchalkov, *Phys. Rev. Lett.* **94**, 057003 (2005).